Respiratory Research

RESEARCH

Open Access

Protease-activated receptor-2 (PAR2) mutation attenuates airway fibrosis in mice during the exacerbation of house dust mite-induced allergic lung disease by multi-walled carbon nanotubes

Logan J. Tisch[1], Ryan D. Bartone[1], Silvio Antoniak[2] and James C. Bonner[1*]

Abstract

Background Pulmonary exposure to multi-walled carbon nanotubes (MWCNTs) induces potent pro-inflammatory and pro-fibrotic responses in mouse models of allergic lung disease. We recently reported that MWCNTs exacerbated components of house dust mite (HDM)-induced allergic lung disease, including eosinophilic inflammation, mucous cell metaplasia and airway fibrosis. Protease-activated receptor 2 (PAR2) plays a significant role in the development of various respiratory diseases, including asthma and pulmonary fibrosis. However, studies investigating the function of PAR2 in allergic lung disease have produced variable results. To further define the role of PAR2 in pulmonary pathology, we investigated the effects of MWCNTs on HDM-induced allergic lung disease in PAR2-mutant mice.

Methods The PAR2-mutant mice used were previously generated by replacing a 1.8-kb region of the PAR2 coding sequence with a neomycin resistance gene, which did not entirely delete the gene. Wild-type (WT) male C57BL/6J mice and PAR2-mutant male mice were exposed to a vehicle solution, MWCNTs, HDM extract, or both via oropharyngeal aspiration six times over 3 weeks. Bronchoalveolar lavage fluid (BALF) was collected to measure changes in inflammatory cells, total protein, and lactate dehydrogenase (LDH). Lung protein and mRNA were assayed for pro-inflammatory and profibrotic mediators, and formalin-fixed lung sections were evaluated for histopathology.

Results In WT and PAR2-mutant mice, co-exposure to MWCNTs and HDM extract significantly increased eosinophilic lung inflammation, mucous cell metaplasia, increased BALF cellularity, BALF total protein, and LDH levels. These results were not significantly different between genotypes. Additionally, MWCNTs and HDM extract co-exposure significantly increased airway fibrosis in WT and PAR2-mutant mice, characterized by increased airway collagen deposition and *Col1a1* mRNA expression. Quantitative morphometry revealed a significant decrease in airway fibrosis in PAR2-mutant mice compared to WT mice, accompanied by reduced *Col1a1* mRNA as detected by PCR. Despite this reduction, the pro-fibrotic mediator arginase 1 (Arg-1) protein and mRNA levels were significantly upregulated in PAR2-mutant mice.

Conclusion Our study demonstrates that PAR2 mediates airway fibrosis but does not influence eosinophilic lung inflammation or mucous cell metaplasia caused by co-exposure to MWCNTs and HDM allergen.

Keywords Allergens, Nanoparticles, Allergic lung disease, Asthma, PAR2

*Correspondence:
James C. Bonner
jcbonner@ncsu.edu
Full list of author information is available at the end of the article

Introduction

Allergic asthma is a respiratory disease caused by genetic predisposition and environmental exposure to allergens, that affects over 300 million people globally. Over the past decade, asthma prevalence has risen, heightening concerns about this chronic disease [1]. Research has increasingly focused on the exacerbation of asthma, as environmental factors can amplify the pathological features of allergic lung disease and worsen debilitating symptoms such as bronchoconstriction. For example, acute viral and bacterial respiratory infections are known to exacerbate allergic asthma [2, 3]. Additionally, inhalation of airborne particles, including ultrafine particulate matter from natural or anthropogenic sources, can lead to prolonged asthma exacerbation [4, 5]. Studies using murine models with house dust mite (HDM) extracts from *Dermatophagoides pteronyssinus* have shown that inhaled particles worsen allergic lung disease by increasing eosinophilic inflammation, mucous cell metaplasia, and airway fibrosis [6]. Therefore, inhaled particles are a major environmental factor contributing to increased severity and exacerbation of allergic lung disease.

Engineered nanomaterials (ENMs) are a significant concern to human pulmonary health due to their small size (10–100 nm) and ability to infiltrate deep within the lungs when inhaled [7]. Multi-walled carbon nanotubes (MWCNTs), a type of ENM, possess unique physicochemical properties, such as high tensile strength and surface functionalization, making them an attractive material for diverse applications, including industrial coatings, light-weight composites, and electronics [8]. The toxicity of MWCNTs is in part due to their fiber-like structure which promotes deep penetration of lung and subpleural tissues following inhalation with subsequent activation of innate immune cells such as macrophages, leading to lung injury [9, 10]. Additionally, inhalation of MWCNTs alone induces systemic immunosuppression and causes interstitial fibrosis in the lungs of mice, potentially mediated by upregulation of TGF-β1 production [11]. Recent studies examining experimental animal models of allergic asthma have revealed that pulmonary exposure to MWCNTs, in combination with HDM allergens, amplifies airway inflammation, fibrosis, and the production of pro-inflammatory cytokines, thus exacerbating allergic lung disease [6, 12–14]. While MWCNT inhalation alters and exacerbates the allergic immune response to allergens, the mechanisms by which these particles enhance allergen-induced lung disease are not well understood.

The protease-activated receptor 2 (PAR2) is a cell surface G-protein-coupled receptor (GPCR) expressed by various lung cell types, including bronchial and alveolar epithelial cells, resident alveolar macrophages, and fibroblasts. PAR2 plays a crucial role in sensing the extracellular proteolytic environment [15, 16]. Endogenous serine and cysteine proteases such as tryptase, trypsin, factor VIIa, factor Xa, and elastase, released or generated during lung injury, cleave PAR2, leading to receptor activation and downstream signaling [17, 18]. Furthermore, PAR2 can be proteolytically activated by the proteases found in HDM, such as Der p1, Der p3, and Der p9 [19, 20]. These proteases cleave the receptor within the extracellular N-terminus, exposing a peptide-tethered ligand domain that binds to conserved regions on PAR2, activating the receptor [21, 22]. This interaction triggers conformational changes and alters the receptor's affinity for intracellular G proteins, mediating downstream receptor signaling. Importantly, PAR2 contains multiple N-terminal cleavage sites with preferential protease binding, leading to protease-specific cellular responses via the same receptor [22]. The prevalence and multifaceted role of PAR2 in the lung microenvironment implicate it in the pathogenesis of various respiratory diseases, including chronic obstructive pulmonary disease (COPD), pulmonary fibrosis, and asthma [23]. The complex nature of PAR2 has made it challenging to elucidate its precise role in the pathogenesis of various inflammatory and immune diseases.

Studies on PAR2 in mice have produced variable results regarding its role in the pathogenesis of allergic lung diseases. Our group previously examined the role of PAR2 in the exacerbation of HDM-induced allergic lung disease by MWCNTs using PAR2 knockout (KO) mice, a complete gene deletion of the receptor [6]. We found that co-exposure to MWCNTs and HDM extract synergistically increased eosinophil numbers in bronchoalveolar lavage fluid (BALF) with no significant differences between wild-type (WT) and PAR2 KO mice. Interestingly, mice exposed to MWCNTs or HDM extract alone showed no discernable differences in collagen deposition. However, quantitative morphometry of trichome-positive histopathological lung sections revealed that co-exposure to MWCNTs and HDM extract significantly increased collagen deposition around airways and pulmonary blood vessels, with WT mice developing significantly more airway fibrosis than PAR2 KO mice [6]. This data suggests that PAR2 activation contributes to pulmonary fibrosis development but does not mediate the exacerbation of HDM-induced eosinophilic lung inflammation by MWCNTs. In contrast, previous research has indicated that PAR2 may regulate cellular motility and airway inflammation. For example, the administration of PAR2 agonist peptides has been reported to reduce lipopolysaccharide (LPS)-stimulated neutrophilia in murine airways, suggesting an anti-inflammatory mechanism for PAR2 [16]. However, it has also been reported that administering a

PAR2-blocking peptide before allergen exposure inhibits airway hyper-responsiveness and inflammation, suggesting that PAR2 signaling mediates the immune response in allergic asthma [24]. Additionally, the role of PAR2 in airway fibrosis has been debated. For instance, PAR2 deficiency achieved by a homozygous null mutation in the *Par2* gene, which reduces the 8-kb gene to a 5-kb gene, did not affect bleomycin-induced lung fibrosis [25, 26]. In contrast, mice with complete gene deletion of PAR2 showed significantly reduced bleomycin-induced pulmonary fibrosis [27]. These differences in the fibrotic response to bleomycin may be attributed to incomplete versus complete gene deletion.

The effects of PAR2 on airway inflammation and the pathogenesis of allergic lung disease remain unclear. Conflicting evidence suggests that PAR2 activation may either promote or protect against the development of allergic lung disease and associated airway fibrosis. We propose these discrepancies can be attributed to variations in PAR2 activation sites or by differences in PAR2-deficient models. As mentioned previously, PAR2 can induce protease-specific cellular responses depending on the site of protease cleavage [22, 28]. It has also been shown that receptor functionality can persist in incomplete knockout models [28, 29]. In the current study, we evaluated the exacerbation of HDM-induced allergic lung disease by MWCNTs in a genetically modified PAR2-mutant mouse model. We hypothesized that the PAR2-mutant mice in this study would exhibit different pathological responses in the exacerbation of HDM-induced allergic lung disease by MWCNTs compared to our previous work with PAR2 KO mice generated by total gene deletion [6, 21]. Similar to our previous findings with PAR2 KO mice, our results in the present study show that MWCNTs exacerbated HDM-induced eosinophilic lung inflammation in both WT and PAR2-mutant mice to the same extent, yet PAR2-mutant mice exhibited significantly reduced trichrome-positive collagen surrounding airways as well as reduced lung *Col1a1* mRNA compared to WT mice after co-exposure to MWCNTs and HDM extract. However, unlike our previous observations with PAR2 KO mice, the reduced airway collagen in the PAR2-mutant mice was accompanied by increased mRNA and protein expression of arginase-1 (Arg-1). In complete PAR2 KO mice, we previously showed that both airway collagen and Arg-1 were significantly decreased [6]. Therefore, both the current study using PAR2-mutant mice and our previous work with PAR2 KO mice support a role for PAR2 in mediating airway fibrogenesis during allergic lung disease. However, the differential expression of Arg-1 in PAR2-mutant mice in this study compared with PAR2 KO mice in our previous work demonstrates some variability in PAR2-deficient mouse models that could shed light on conflicting findings in PAR2-related pulmonary research.

Materials and methods

House dust mite (HDM) extract

HDM extract from *Dermatophagoides pteronyssinus* was purchased from Greer Laboratories Inc. (Lenoir, NC). Lyophilized HDM extract was dissolved in Dulbecco's phosphate buffered saline (DPBS) to achieve a stock total HDM extract protein concentration of 1 mg/mL, with a total yield of 4.57 mg, as measured by Bradford assay. The HDM extract [item #XPB91D3A2.5; lot #390991] contained 1610 endotoxin units (EU), measured by amoebocyte lysate test, according to the manufacturer. Stock solution was further diluted in DPBS to achieve the necessary working concentrations for dosing.

Multi-walled carbon nanotubes (MWCNTs)

MWCNTs (NC7000) were purchased from Nanocyl, Inc. (Sambreville, Belgium) and have been thoroughly characterized previously [30]. MWCNTs were suspended in DPBS (Sigma, St. Louis, MO) to achieve a stock concentration of 3.3 mg/mL. The prepared stock of MWCNTs suspension was sonicated in a cup horn sonicator (Q500, Qsonica, Newtown, CT) for 10 min at 60 amps. The stock solution was diluted with DPBS to achieve a working dosing concentration of 0.25 mg/mL. Mice were dosed with MWCNTs via oropharyngeal aspiration (OPA) in the presence or absence of HDM extract.

Mice

WT male C57BL/6J mice and PAR2-mutant male mice (8–12 weeks) were used for this study [31]. The PAR2-mutant mice were originally generated at the R.W. Johnson Pharmaceutical Research Institute, Spring House, PA. Dr. Antoniak established a colony after receiving PAR2-mutant mice from Dr. Nigel Mackman (University of North Carolina at Chapel Hill). The WT and PAR2-mutant mice were bred as cousin lines to reduce unnecessary euthanasia of heterozygote PAR2-mutant mice. A schematic illustration of the targeting vector used to generate the PAR2-mutant mice is shown in Fig. 1A, which results in a higher mobility shift in the PAR2 gene but not a complete gene deletion. Briefly, a 1.8-kb *Hind*III-*Sal*I region that covers part of intron 1 and exon 2 was deleted and replaced with a neomycin-resistance gene [31]. These mice have previously been shown to have reduced lung inflammation induced by influenza, reduced cardiac ischemia/reperfusion injury, and reduced renal fibrosis following unilateral ureteric obstruction [32–34]. In these previous studies, the mice are referred to as PAR2-deficient or $PAR2^{-/-}$ mice. We refer to these mice as

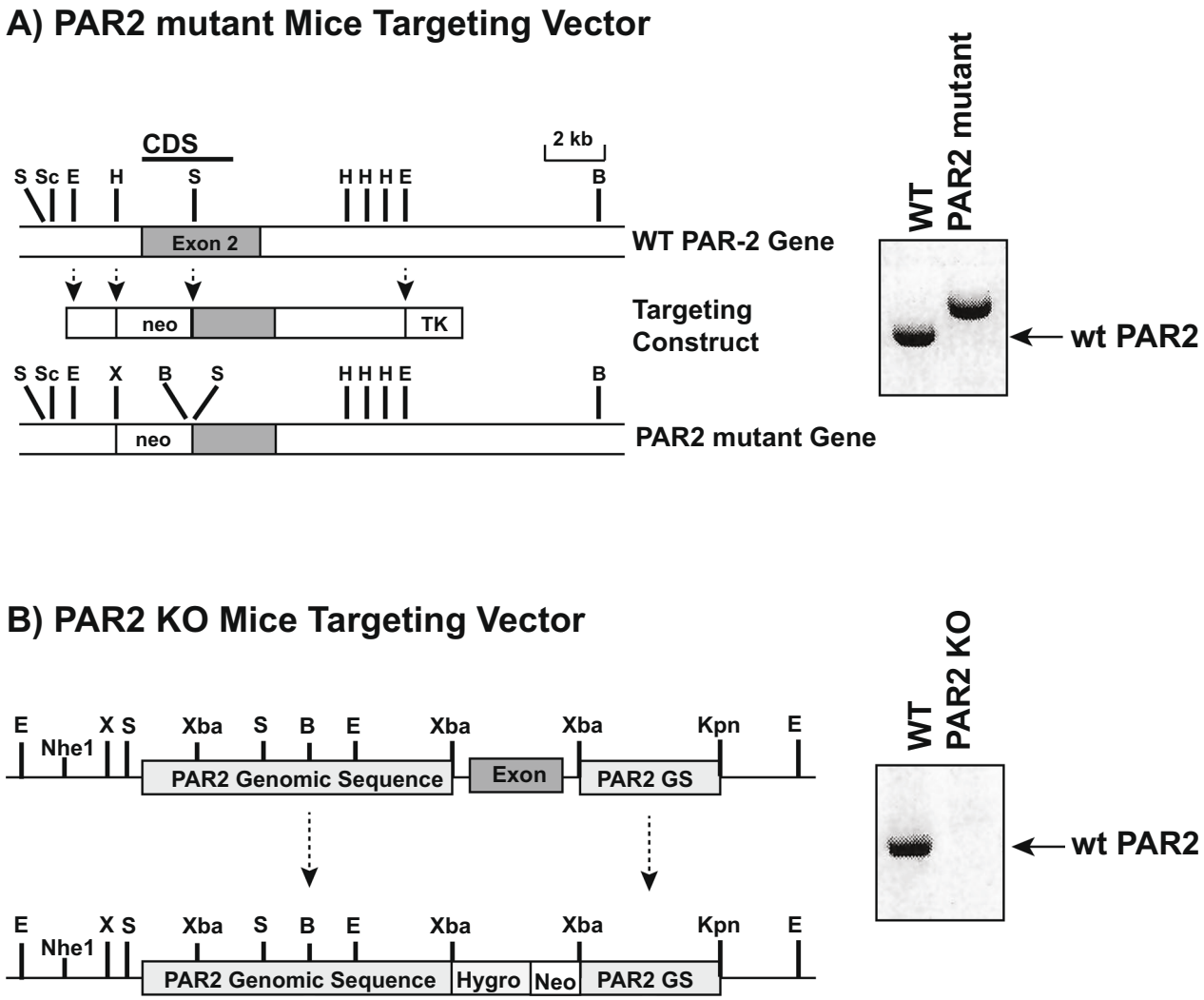

Fig. 1 Schematic illustrations showing generation of targeting vectors for (**A**) PAR2 mutant mice used in the current study (adapted from ref. 31). Side panel shows PCR genotyping results from WT and PAR2 mutant mice. **B** PAR2 KO mice from Jackson Laboratories (adapted from ref. 21). Side panel shows PCR genotyping results from WT and PAR2 KO mice

"PAR2-mutant" in the current study since they possess a partial gene deletion, which differentiates them from PAR2 KO mice that possess a complete gene deletion [6]. Genotyping of all mice used in this study is shown in Supplementary File 1. In contrast to the PAR2-mutant mice which have an incomplete gene deletion, Fig. 1B illustrates the targeting vector used to generate PAR2 KO mice (B6.Cg-F2rl1tm1Mslb/J) from the Jackson Laboratory (Bar Harbor, ME) we previously investigated [6]. These PAR2 KO mice have a total deletion of the PAR2 gene as shown by PCR genotyping (Fig. 1B).

Animal care

Mice were housed in an AAALAC (Association for Assessment and Accreditation of Laboratory Animal Care) accredited animal facility. All animal procedures were approved by the NC State University Institutional Animal Care and Committee (IACUC). Mice were housed in five per cage according to their respective treatment groups and genotypes-vehicle control (WT), vehicle control (PAR2-mutant), MWCNTs (WT), MWCNT (PAR2-mutant), HDM extract (WT), HDM extract (PAR2-mutant), MWCNTs + HDM (WT), MWCNTs + HDM (PAR2-mutant).

Exposure of mice to MWCNTs and HDM extract

Exposure procedures consisted of three sessions in the sensitization phase (days 1, 3, 5) and the challenge phase (days 15, 17, 19). Mice were exposed by OPA to 50 µL of the following treatments: vehicle solution control,

MWCNTs, HDM extract, or both. Treatments were prepared in a vehicle solution consisting of DPBS and were vortexed immediately before delivery to mice under isoflurane anesthesia. WT and PAR2-mutant mice were exposed to vehicle control or 0.5 μg/mouse HDM extract (0.02 mg/kg) per dosing session with or without 12.5 μg of MWCNTs (0.5 mg/kg). Total doses of 0.12 mg/kg HDM extract and 3 mg/kg MWCNTs were delivered throughout the sensitization period.

Necropsy and tissue collection

Necropsy was performed on day 22 for sample collection. Mice were euthanized with an intraperitoneal injection of pentobarbital. Bronchoalveolar lavage fluid (BALF) was collected from each mouse by cannulating the trachea and conducting lavages of the lungs with 0.5 mL of chilled DPBS two times. BALF was utilized to analyze protein, lactate dehydrogenase LDH, and cytokines/chemokines. For histopathology, the left lung lobe was fixed in neutral buffered formalin (VWR, Radnor, PA) for 24 h, then transferred to 70% ethanol for a week before being embedded in paraffin. A right superior lung lobe was stored in RNAlater (Fisher Scientific, Waltham, MA) at − 80 °C for mRNA analysis. The right medial and inferior lung lobes were snap-frozen in liquid nitrogen and stored at − 80 °C for protein analysis.

Analyses of BALF

Total BALF cell counts were performed using a hemacytometer. For differential cell counts, 100 μL of BALF was centrifuged onto glass slides using a Cytospin 4 centrifuge (ThermoFisher, Waltham, MA). Slides were then fixed and stained with the Diff-Quik stain set (Epredia, Kalamazoo, MI). Cell differentials were quantified by counting 500 cells per slide using an Olympus light microscope BX41 (Center Valley, PA) to determine relative numbers of macrophages, neutrophils, eosinophils, and lymphocytes.

Cytokine analysis in BALF

To measure cytokines in BALF, DuoSet enzyme-linked immunosorbent assay (ELISA) kits (R&D Systems, Minneapolis, MN) were used according to the manufacturer's protocol to quantify protein levels of cytokines C-X-C motif chemokine ligand 1 (CXCL1) and CC motif chemokine ligand 11 (CCL11) from BALF. BALF cytokine absorbances were measured using the Multiskan EX microplate spectrophotometer (ThermoFisher, Waltham, MA). Measured absorbances were then used to calculate cytokine concentrations using GraphPad Prism, version 10.0 (La Jolla, CA).

Cytotoxicity and total protein in BALF

LDH activity in BALF was measured as an indicator for pulmonary cytotoxicity with the Pierce LDH Cytotoxicity Assay Kit (ThermoFisher, Waltham, MA), according to the manufacturer's instructions. The Pierce BCA Protein Assay Kit (ThermoFisher) was used to determine the total protein concentration in BALF.

qRT-PCR

Applied Biosystems high-capacity cDNA reverse transcription kit (ThermoFisher Scientific, Waltham, MA) was used to generate cDNA from the mRNA isolated from the right lung lobe using Quick-RNA™ MiniPrep (Zymo Research, Irvine, CA) according to the manufacturer's instructions. The FastStart Universal Probe Master (Rox) (Roche, Basel, Switzerland) was used to run Taqman qPCR on the Applied Biosystems QuantStudio3 Real-Time PCR System Thermal Cycling Block (ABI, Foster City, CA) to determine the comparative C_T ($\Delta\Delta C_T$) fold change expression of specific mRNAs (*Col1a1*, *Arg1*, *Muc5ac*, *Ccl-11*) normalized to β2 microglobulin *B2M* as the endogenous control. qRT-PCR primers were purchased from ThermoFisher Scientific (*Col1a1*, #Mm00801666_g1; *Arg1*, #Mm00475988_m1; *Muc5ac*, #Mm01276718_m1; *Ccl-11*, #Mm00441238_m1; *B2M*, #Mm00437762_m1).

Immunoblotting

Whole lung lysate was prepared from snap-frozen right lung lobes. Frozen samples were digested using lysis buffer (20 mM Tris–HCl, 150 mM NaCl, 1 mM EDTA, 1 mM EGTA, 1% Triton X-100, 1 mM Na_3VO_4, 1×Halt™ Protease Inhibitor Cocktail, in DPBS). Samples were digested using a Mini Bead Mill Homogenizer (VWR International). The protein concentration of the supernatant was determined using the Pierce BCA Protein Assay Kit (ThermoFisher Scientific, Waltham, MA). Samples were loaded onto a Mini-PROTEAN TGX 4–15% SDS-PAGE gel (Bio-Rad Laboratories Inc., Hercules, CA), separated by electrophoresis and transferred onto PVDF membranes. Membranes were blocked and incubated in mouse primary antibodies purchased from Cell Signaling Technology (phosphorylated STAT6 at Tyr640, #56554S; STAT6, #5397S; Arginase-1, #93668S; and β-actin, #4967L). Following primary antibody incubation, membranes were incubated with horseradish peroxidase-conjugated (HRP) secondary anti-rabbit antibody (Cell Signaling Technology, Danvers, MA). Enhanced chemiluminescence (ECL) Prime Western Blotting Detection Reagent (Cytiva, Marlborough, MA) was used to facilitate HRP-induced chemiluminescence according to the manufacturer's instructions. Resulting signals were captured using Amersham Imager 680 (GE Life Sciences, Marlborough, MA), and semi-quantitative

densitometry was performed using ImageQuant software (GE Life Sciences, Marlborough, MA).

Histopathology

The left lung was cut into three cross sections, which were embedded in paraffin, and 5-micron histologic sections were mounted on charged glass slides. Sections were stained with Masson's trichrome for collagen deposition or Alcian blue/periodic acid-Schiff (AB/PAS) for mucus production.

Quantitative morphometry of airway fibrosis and mucous cell metaplasia

Based on Masson's trichrome-stained slides, airway fibrosis was assessed by measuring the collagen layer's thickness surrounding the airways using an area/perimeter ratio method, as described previously [6, 35]. Approximately 10 airways per lung cross-sections per mouse (3 cross-sections per mouse, resulting in a total of 30 photomicrographs per mouse) that fit our criteria (circular airways that fit in the field of view) were photographed at 100×magnification using an Olympus BX41 light microscope (Center Valley, PA). To determine the area/perimeter ratio, round to oval-shaped airways under 500×500 µm (H×W) were imaged at 100×. The lasso tool in Adobe Photoshop CS5 was used to surround trichrome-positive collagen around the airways, giving the outer area, and to surround the basement membrane, giving the inner area and circumference (perimeter). The difference between the outer and inner area was divided by the circumference, which gave the area/perimeter ratio. All measurements were performed in a blinded manner. Mucous cell metaplasia and airway mucus production were assessed by imaging all airways under approximately 500×500 µm (H×W) in each AB/PAS-stained sample and quantifying the area of positive staining in ImageJ (National Institutes of Health) as a percent area.

Statistical analysis

One-way ANOVA with Tukey's post hoc test or Student's t-test was used to evaluate differences between treatment groups (GraphPad Prism, version 10.0, La Jolla, CA). Two-way ANOVA with Tukey's post hoc test was utilized to evaluate differences among treatment and sex groups. All data represent the mean ± SEM of four to five animal replicates.

Results

Pulmonary co-exposure to MWCNTs and HDM extract increases lung inflammation and results in eosinophilic infiltration

Using the sensitization and challenge protocol illustrated in Fig. 2A, male C57BL/6J WT and PAR2-mutant mice were exposed by OPA 6 times over 3 weeks. Treatment groups included 50 µL of DPBS solution as the vehicle control, 12.5 µg of MWCNTs (0.5 mg/kg), 0.5 µg of HDM extract (0.02 mg/kg), or a combination of MWCNTs and HDM per dosing session as described in the Materials and Methods section. Analysis of BALF showed that co-exposure of MWCNTs and HDM extract significantly increased the total number of cells, which was similar between WT and PAR2-mutant mice (Fig. 2D). Accordingly, MWCNT and HDM co-exposure significantly increased total protein and LDH in BALF with no observable differences between WT and PAR2-mutant mice (Fig. 2B and C). Cytospins slides of mouse BALF cells demonstrated that MWCNTs and HDM extract co-exposure initiated a substantial increase in eosinophils compared to either MWCNT or HDM extract alone (Fig. 2E). Differential cell counting of BALF cells confirmed that mice co-exposed with MWCNTs and HDM extract were the only treatment group that exhibited a significant increase in eosinophil numbers (Fig. 2G). On the other hand, MWCNT and HDM co-exposure significantly decreased macrophage numbers in WT and PAR2-mutant BALF (Fig. 2F), primarily due to increased infiltrating eosinophils. Additionally, there were no significant differences in the numbers of neutrophils in BALF between genotypes or treatment groups (Fig. 2H). These data demonstrated that co-exposure with MWCNT and HDM extract significantly increases eosinophil infiltration within the lungs of mice compared to either treatment alone. Additionally, no differences were observed between genotypes, suggesting that the mutation of PAR2 did not significantly contribute to inflammatory cell recruitment following MWCNT and HDM extract exposure.

PAR2 contributes to the exacerbation of airway fibrosis induced by co-exposure to MWCNTs and HDM extract

Pulmonary fibrosis in the lungs of exposed mice was evaluated by quantitative morphometry of Masson's trichrome-staining airway collagen using the area-perimeter ratio method described in the Materials and Methods section. While no observable differences were seen between genotypes from groups exposed to either HDM extract or MWCNTs alone, PAR2-mutant mice displayed a significant increase in trichrome-positive collagen around airways in the lungs of treated mice compared to the vehicle control group (Fig. 3A). Additionally, co-exposure to MWCNTs and HDM extract further increased trichrome-positive collagen in both WT and PAR2-mutant mice compared to either HDM extract or MWCNTs alone (Fig. 3A). Quantitative morphometry of trichrome-positive airway collagen revealed a significant increase in airway fibrosis in WT

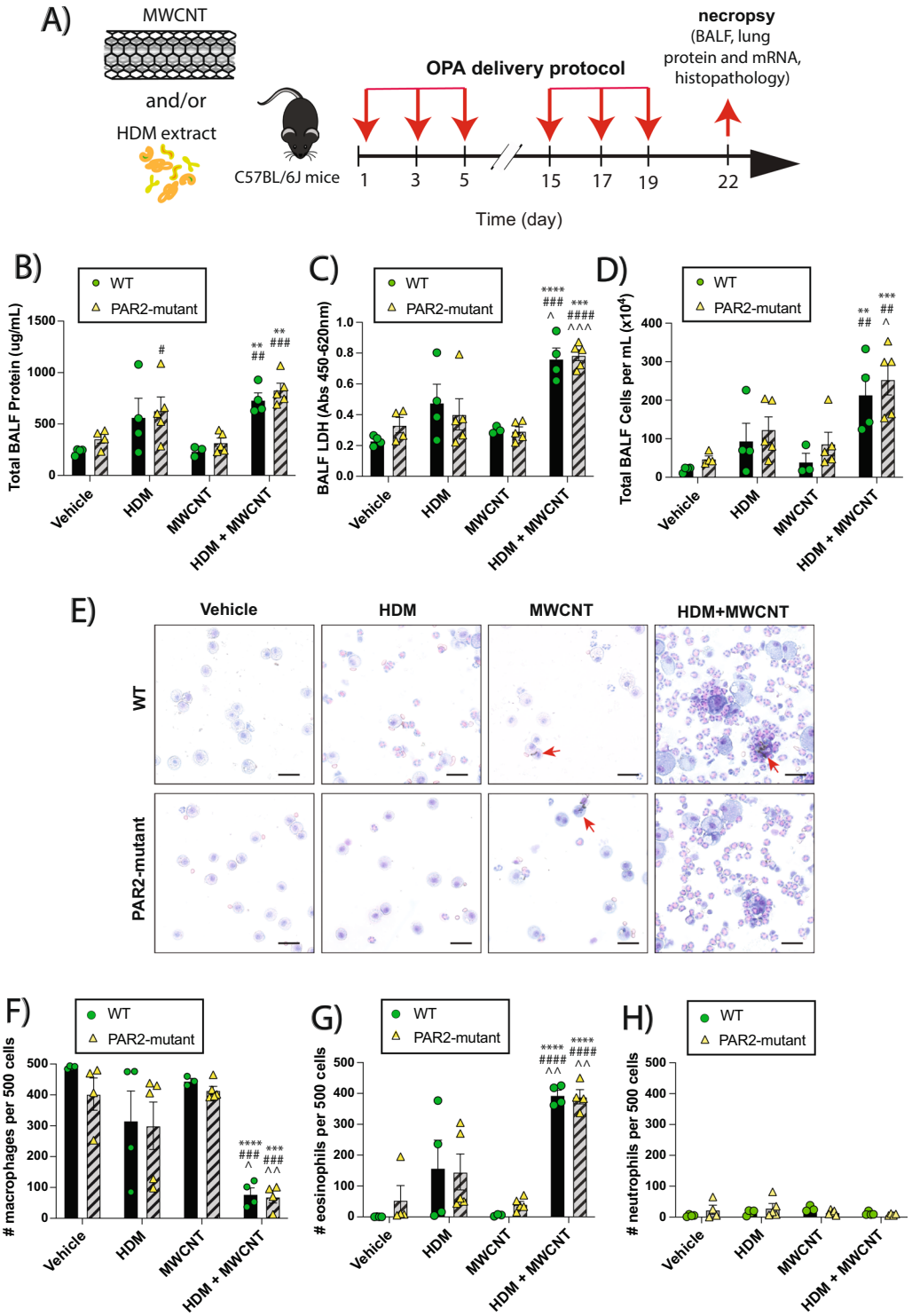

Fig. 2 Cellularity and biomarkers of lung injury in BALF from mice exposed to HDM extract, MWCNTs or both. **A** Illustration of the exposure protocol. **B**–**D** Total protein, LDH and total cell counts in BALF. **E** Cytospin images from BALF showing eosinophilic inflammation after co-exposure to MWCNTs and HDM extract. Red arrows indicate macrophages with MWCNT inclusions. Black bars = 10 µm. **F**–**H** Differential cell counts from Cytospins showing macrophages, eosinophils and neutrophils. $^{**}p < 0.01$, $^{***}p < 0.001$, $^{****}p < 0.0001$ compared to vehicle; $^{\#}p < 0.05$, $^{\#\#}p < 0.01$, $^{\#\#\#}p < 0.001$, $^{\#\#\#\#}p < 0.0001$ compared to MWCNTs; $^{\wedge}p < 0.05$, $^{\wedge\wedge}p < 0.01$, $^{\wedge\wedge\wedge}p < 0.001$ compared to HDM extract determined by two-way ANOVA with Tukey's post-hoc test

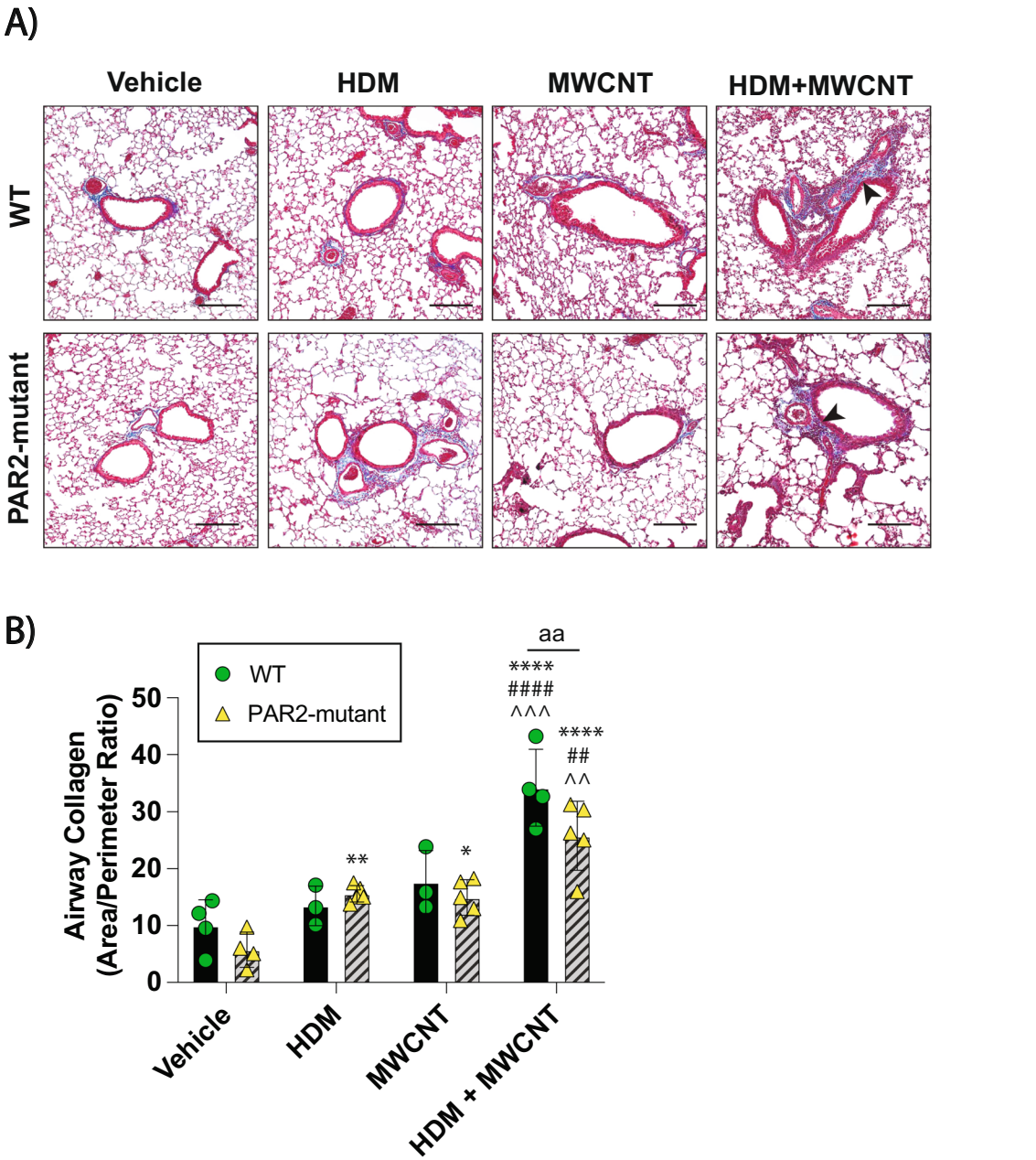

Fig. 3 Airway fibrosis in the lungs of wildtype (WT) and PAR2-mutant mice exposed to MWCNTs in the absence or presence of HDM extract. **A** Representative images of trichrome-stained lung tissue sections showing blue collagen deposits (arrowheads). Black bars = 100 µm. **B** Morphometric quantification of airway collagen using area-perimeter method. $^{****}p < 0.0001$ compared to vehicle; $^{\#\#}p < 0.01$, $^{\#\#\#\#}p < 0.0001$ compared to MWCNT treatment; $^{\wedge\wedge}p < 0.01$, $^{\wedge\wedge\wedge}p < 0.001$ compared to HDM treatment; $^{aa}p < 0.01$ between genotypes as determined by two-way ANOVA with Tukey's post-hoc test

mice co-exposed to both MWCNTs and HDM extract when compared to PAR2-mutant mice (Fig. 3B). AB-PAS staining was performed on lung tissues to detect mucous cell metaplasia in the lungs of mice. Photomicrographs of AB-PAS-stained lung sections showed significantly increased AB-PAS staining indicative of mucous cell metaplasia in mice co-exposed to MWCNTs and HDM extract (Fig. 4A). However, quantitative morphometry revealed that there were no significant differences between WT and PAR2-mutant mice (Fig. 4B). Together these results indicate that PAR2 is required for increased airway fibrosis but not

mucous cell metaplasia that is associated with MWCNTS and HDM extract induced pathology.

Co-exposure to MWCNTs and HDM extract upregulates signaling components of the immune response

Next, we assessed the effects of MWCNTs and HDM extract on the inflammatory and fibrotic responses in the lungs of WT and PAR2-mutant mice by ELISA and qRT-PCR. Lung BALF from treated mice revealed that the neutrophil chemokine CXCL1 was significantly upregulated in WT mice exposed to HDM extract alone or in combination with MWCNTs compared to the vehicle control (Fig. 5A). The observed response in WT mice was significantly greater compared to PAR2-mutant mice (Fig. 5A). Additionally, there were no significant differences in treatment groups or genotypes for the eosinophil

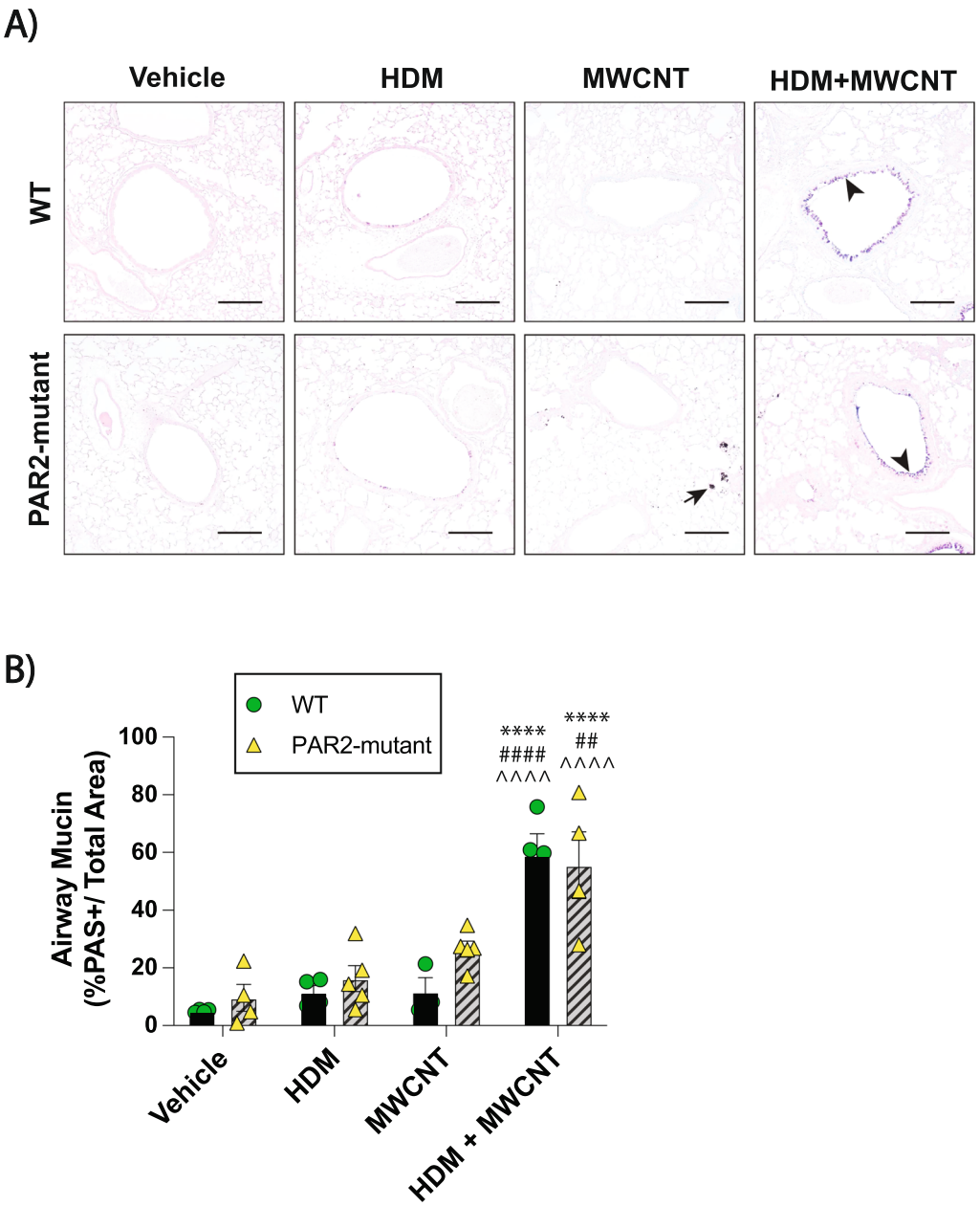

Fig. 4 Mucous cell metaplasia in the lungs of wildtype (WT) and PAR2-mutant mice exposed to MWCNTs in the absence or presence of HDM extract. **A** Representative images of AB-PAS-stained lung tissue sections positive for PAS + mucins stained purple (arrowheads). Arrows indicate MWCNTs. Black bars = 100 µm. **B** Morphometric quantification of AB-PAS + airway mucin. $^{****}p < 0.0001$ compared to vehicle; $^{\#\#}p < 0.01$, $^{\#\#\#\#}p < 0.0001$ compared to MWCNT treatment; $^{\wedge\wedge\wedge\wedge}p < 0.0001$ compared to HDM treatment as determined by two-way ANOVA with Tukey's post-hoc test

chemotactic CCL11 (Fig. 5B). qRT-PCR analysis revealed significantly increased *Col1a1* mRNA levels after co-exposure to MWCNT and HDM extract groups for both genotypes, yet there were no significant differences in MWCNT or HDM extract groups alone (Fig. 6A). PAR2-mutant mice had significantly lower *Col1a1* mRNA compared to WT mice (Fig. 6A). The mRNA expression of *Arg-1*, a T_H2 molecule and marker of alternatively activated macrophages, was also significantly increased in the MWCNT and HDM extract co-exposure group in WT and PAR2-mutant mice compared to the vehicle control (Fig. 6B). Notably, *Arg-1* expression was significantly increased in PAR2-mutant versus WT mice upon HDM and MWCNT co-exposure (Fig. 6B). The mRNA expression of *Ccl11* in WT mice co-exposed to HDM extract and MWCNTs increased significantly compared to vehicle and MWCNT control groups. There were no statistical differences in *Ccl11* mRNA expression in the other treatment groups (Fig. 6D). The mRNA expression of *Muc5ac* was not significantly different among treatment groups or genotypes (Fig. 6C).

PAR2 regulates a T_H2 type immune response

Whole lung lysates were evaluated by Western blot analysis to investigate specific molecular mechanisms that contribute to the exacerbation of the lung inflammatory or fibrotic response induced by HDM extract and MWCNT co-exposure. Western blots from all animals evaluated are shown in Fig. 7A. Uncropped Western blots are shown in Supplementary File 2. Co-exposure to MWCNTs with HDM extract increased Arg-1 protein expression in WT and PAR2-mutant mice, although expression was markedly elevated in PAR2-mutant mice (Fig. 7A, C). Additionally, MWCNT and HDM extract co-exposure increased the phosphorylation of STAT6 in one out of four WT mice and three out of five PAR2-mutant mice, while total STAT6 remained relatively constant among treatments and genotypes. However, due to animal variation, densitometric analysis revealed no significant differences between treatment groups or genotypes for pSTAT6 expression (Fig. 7B).

Discussion

Understanding the mechanisms through which inhaled nanoparticles exacerbate allergen-induced lung disease in experimental animal models is critical to uncovering how such particles influence the pathogenesis of asthma in humans. Our group previously demonstrated that MWCNTs, in the presence of HDM extract, exacerbate allergen-induced responses by increasing serum IgE levels, airway fibrosis, and inducing mucous cell metaplasia [36]. Recent work by our group using mice with complete PAR2 gene deletion (i.e., PAR2 KO mice) demonstrated that PAR2 was not involved in eosinophilic lung inflammation but contributed to airway fibrogenesis [6]. However, the literature presents conflicting findings on the role of PAR2 in allergic lung disease and fibrogenesis, with studies using complete and partial knockout models reporting variable outcomes [21, 25]. In the current study, we aimed to clarify these discrepancies by using

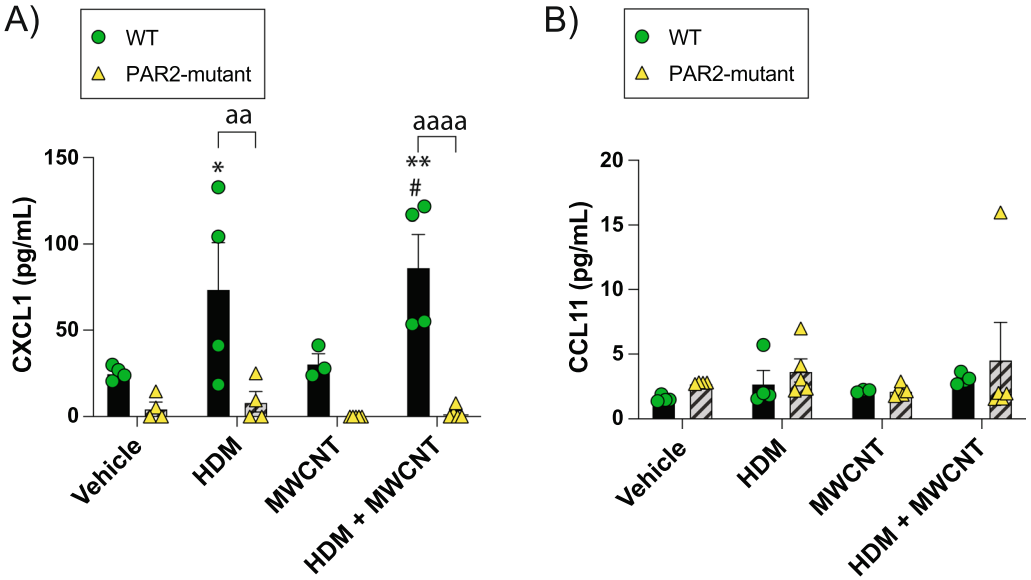

Fig. 5 Protein levels of **A** CXCL1 and **B** CCL11 in the BALF of wildtype (WT) and PAR2-mutant mice exposed to MWCNTs in the absence or presence of HDM extract. $^{*}p < 0.05$, $^{**}p < 0.01$ compared to vehicle; $^{\#}p < 0.05$ compared to MWCNT treatment; $^{aa}p < 0.01$, $^{aaaa}p < 0.0001$ between genotypes as determined by two-way ANOVA with Tukey's post-hoc test

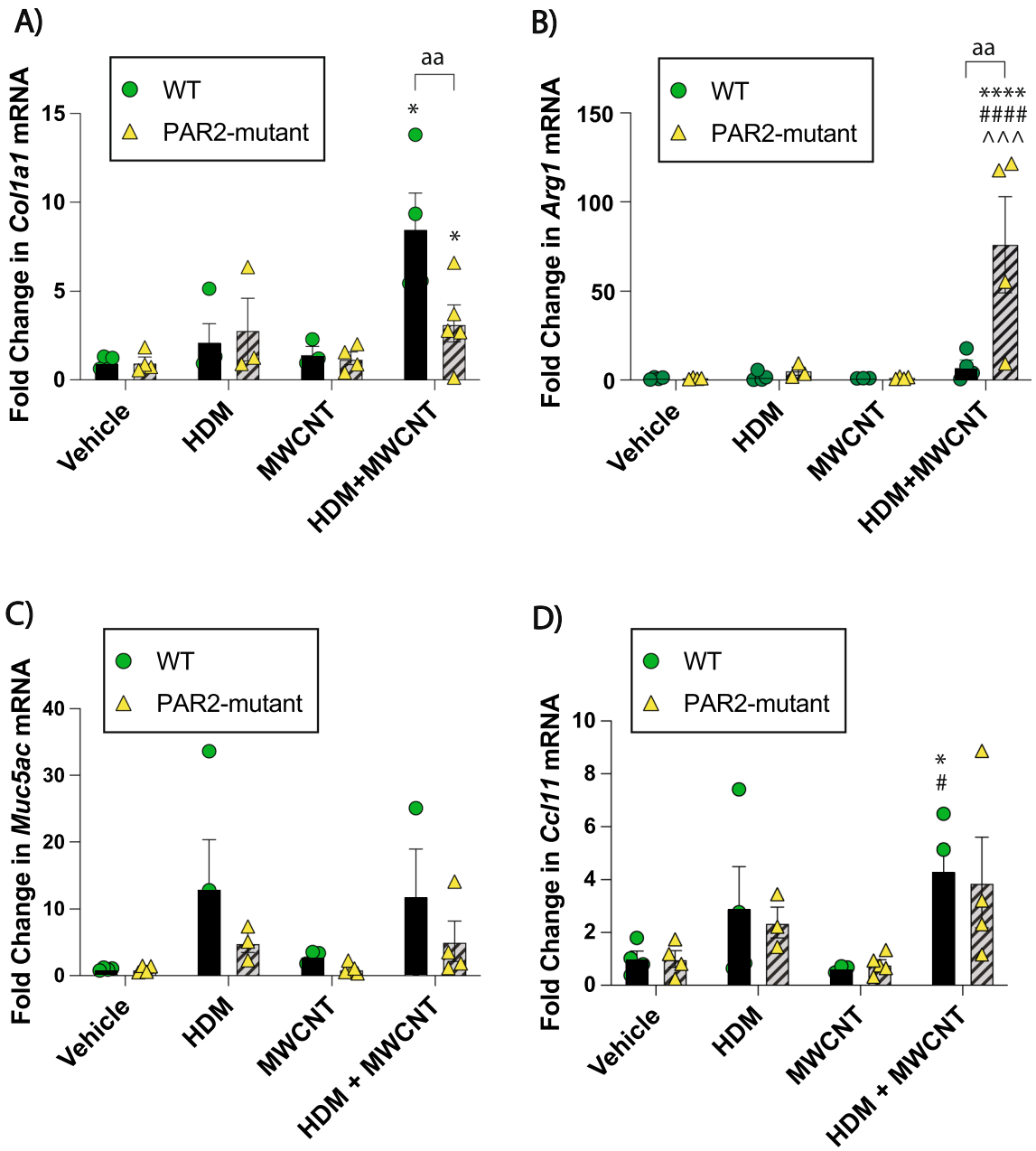

Fig. 6 qRT-PCR of biomarkers of airway inflammation and fibrosis in the lungs of wildtype (WT) and PAR2-mutant mice exposed to MWCNTs in the absence or presence of HDM extract. **A** *Col1a1* mRNA. **B** *Arg1* mRNA. **C** *Muc5ac* mRNA. **D** *Ccl11* mRNA. $^{*}p < 0.05$, $^{****}p < 0.0001$ compared to vehicle; $^{\#}p < 0.05$, $^{\#\#\#\#}p < 0.0001$ compared to MWCNT; $^{\wedge\wedge\wedge}p < 0.001$ compared to HDM; $^{aa}p < 0.01$ between genotypes as determined by two-way ANOVA with Tukey's post-hoc test

PAR2-mutant mice with an partial gene deletion to investigate the impact of MWCNTs on HDM-induced allergic lung disease.

In this PAR2-mutant mouse model, we found that MWCNTs significantly exacerbated allergic responses induced by HDM, marked by elevated eosinophilic infiltration, LDH, and total protein levels in BALF (Fig. 2). Notably, the co-exposure effect occurred despite the use of MWCNT and HDM extract doses that individually elicited low immunological responses. This finding contrasts with a previous study by Schmidlin and colleagues using complete PAR2 KO mice, where a 73% reduction in eosinophil infiltration was observed following ovalbumin sensitization [21]. However, we previously reported that

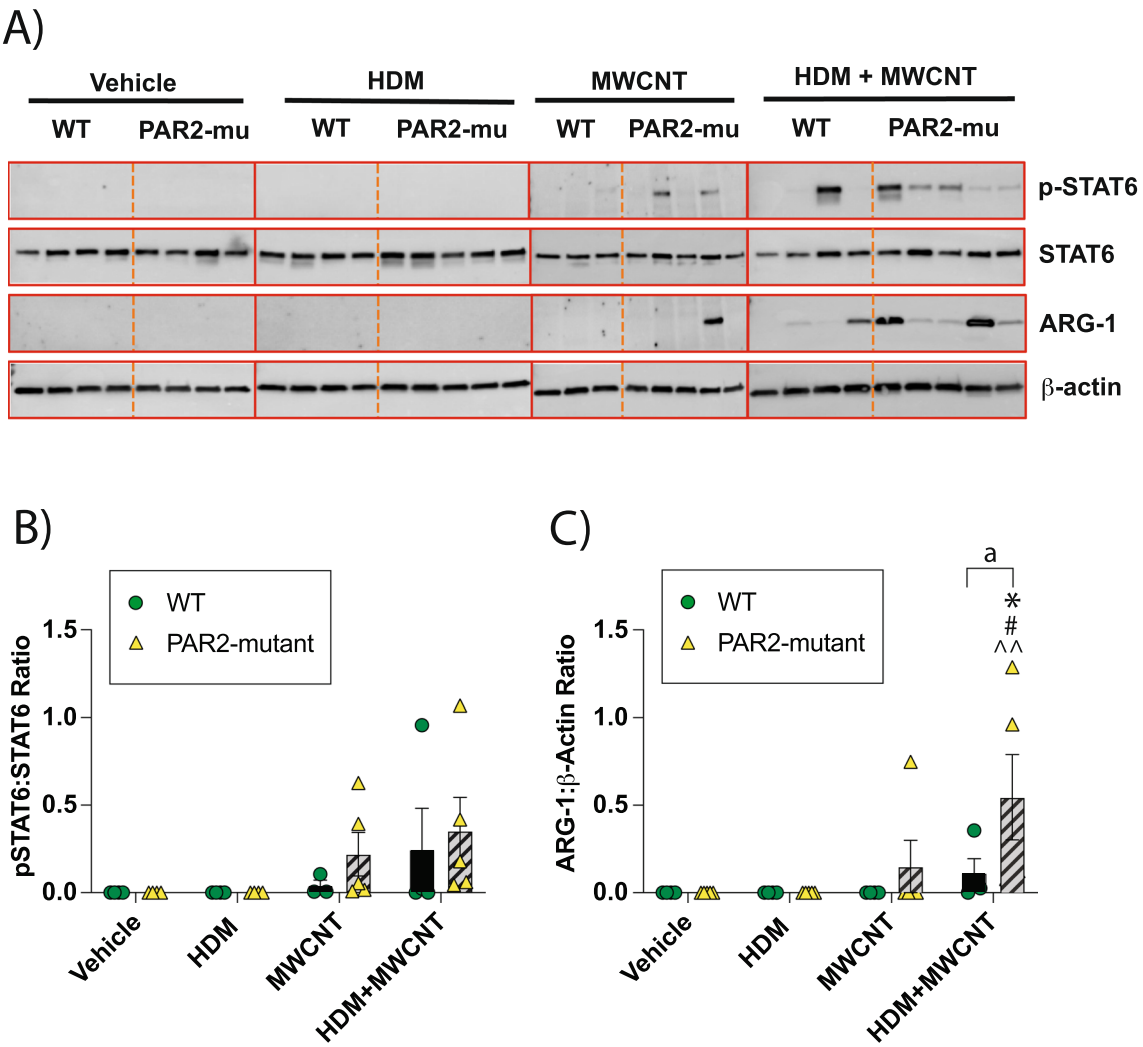

Fig. 7 **A** Western blots of whole lung lysates from wildtype (WT) and PAR2-mutant (PAR2-mu) mice exposed to MWCNTs in the absence or presence of HDM extract. Each lane represents an individual animal. **B** Densitometry of p-STAT6 normalized against total STAT6. **C** Densitometry of ARG-1 normalized to β-actin. $^{*}p < 0.05$ compared to vehicle; $^{a}p < 0.05$ between genotypes as determined by two-way ANOVA with Tukey's post-hoc test

complete PAR2 KO mice had similar BALF eosinophil counts to WT mice [6]. Similarly, in the present study, eosinophilic lung inflammation was not significantly different between WT and PAR2-mutant mice. Additionally, we observed an upregulation of phosphorylated STAT6 in PAR2-mutant mice compared to WT mice co-exposed to MWCNTs and HDM extract (Fig. 7). STAT6 plays a crucial role in eosinophilic lung inflammation. For example, our group's prior research demonstrated that eosinophilic lung inflammation induced by MWCNTs and HDM extract was abolished in STAT6-deficient mice [36]. This finding aligns with our prior results, underscoring the critical role of STAT6 in eosinophil recruitment to the lungs. While this suggests that PAR2 may not directly mediate eosinophilic inflammation, it may influence pathways involved in STAT6 phosphorylation, indicating a more complex role for PAR2 in allergic responses.

Increased mucus production in the lungs is a major contributor to airflow obstruction in asthma and is recognized as a critical indicator of airway remodeling and mucous cell metaplasia [37, 38]. Goblet cells within the respiratory epithelium are the primary source of mucus secreted into the airway lumen following exposure to allergens [39]. In the current study using PAR2-mutant mice, AB-PAS staining revealed a synergistic increase in mucous cell metaplasia following co-exposure to MWCNTs and HDM extract, with no significant differences

between WT and PAR2-mutant genotypes as confirmed by quantitative morphometry. These findings align with our previous results using PAR2 KO mice, where mucous cell metaplasia was similarly increased upon co-exposure, again without significant genotype-based variation. Moreover, prior studies have shown that stimulating human bronchial epithelial cells with synthetic PAR2 agonist peptides only minimally elevated mucus secretion, even at high concentrations [27]. This evidence suggests that PAR2 is limited in regulating mucus hypersecretion during airway inflammation, regardless of receptor manipulation.

The precise function of PAR2 in inflammatory processes remains unclear, as studies have reported both pro- and anti-inflammatory roles depending on the context. For instance, co-activation of PAR2 and Toll-like receptor 4 (TLR4) by a PAR2 activating peptide and LPS in endothelial cells enhanced NF-κB and IL-6 production, suggesting a synergistic pro-inflammatory effect [40]. Conversely, the co-activation of PAR2 and TLR4 in peritoneal macrophages induced an anti-inflammatory response, attenuating LPS-induced pro-inflammatory cytokines (TNF-α, IL-6, IL-12) [41]. Similarly, PAR2 KO mice show reduced IRF gene activation following LPS exposure [42]. These divergent results may be due to variations in the cellular context, tissue type, and specific proteases involved in PAR2 activation [23, 43]. Although we did not observe reduced eosinophil infiltration in PAR2-mutant mice, BALF cytokine analysis revealed a significant reduction in the chemokine CXCL1. Animal studies have implicated CXCL1 in the recruitment and activation of neutrophils, which can exacerbate tissue injury, particularly in the lungs [44]. Dysregulation of CXCL1 is also associated with increased severity of allergic lung disease [45]. Therefore, the downregulation of CXCL1 in PAR2-mutant mice may suggest a potential mechanism by which PAR2 influences lung inflammation, offering new insights into its role in the pathogenesis of allergic lung disease.

Although PAR2 may not directly mediate eosinophilic inflammation, the findings from this study suggest that PAR2 plays a significant role in airway fibrosis. Our previous research demonstrated that total deletion of PAR2 significantly attenuated airway collagen deposition stimulated by co-exposure to MWCNTs and HDM extract [6]. Similarly, in the present study morphometric analysis of lung tissue sections revealed that WT and PAR2-mutant mice exposed to MWCNTs and HDM extract had markedly increased airway collagen compared to vehicle controls, yet PAR2-mutant mice had significantly less airway collagen after co-exposure compared to WT mice. Additionally, *Col1a1* mRNA, a marker of type I collagen, was significantly elevated in WT and PAR2-mutant mice under co-exposure conditions and was significantly reduced in PAR2-mutant mice compared to WT mice. The reduced airway collagen observed in PAR2-mutant in the present study and PAR2 KO mice in our previous work following MWCNT and HDM extract co-exposure reinforces the conclusion that PAR2 actively contributes to the development of pulmonary fibrosis. It is noteworthy that others have shown that the same PAR2-mutant mice used in the present study have been shown to have reduced renal fibrosis following unilateral ureteric obstruction [34]. In that study the authors demonstrated that renal fibrosis was mediated through a mechanism involving PAR2 transactivation of the EGF receptor and the TGF-β receptor. Whether PAR2 mediates lung fibrosis through a similar mechanism remains to be elucidated.

While the attenuation of airway collagen deposition was observed with both PAR2-mutant and PAR2 KO, the present study found that Arg-1 is markedly increased in PAR2-mutant mice compared to WT mice. This contrasts with our previous work with PAR2 KO mice, which showed that *Arg-1* mRNA and protein were significantly decreased in the lungs of PAR2 KO mice compared to WT mice [6]. Therefore, the complete gene deletion in PAR2 KO mice in our previous work versus the mutation of PAR2 in the present work is an important determinant of Arg-1 regulation. A significant contributor to the progression of collagen deposition and fibrosis is the metabolic reprogramming and dysregulation of alveolar epithelial cells, macrophages, fibroblasts, and myofibroblasts, which collectively promote collagen synthesis [46]. A critical precursor of collagen, L-proline, is synthesized from L-arginine by the enzymatic activity of Arg-1. Arg-1 is highly expressed in alveolar macrophages from patients with idiopathic pulmonary fibrosis [46, 47]. Supporting this notion, inhibition of Arg-1 has been shown to reduce collagen deposition and improve outcomes in bleomycin-induced pulmonary fibrosis by suppressing myofibroblast activation [48, 49]. Thus, Arg-1 is often considered a key marker of fibrotic processes [50]. In the present study, we observed that co-exposure to MWCNTs and HDM extract significantly increased Arg-1 protein expression in WT and PAR2-mutant mice, as measured by Western blot analysis. However, the increase in Arg-1 protein levels was particularly pronounced in PAR2-mutant mice. Similarly, *Arg-1* mRNA expression was significantly elevated in WT and PAR2-mutant mice following co-exposure to HDM and MWCNTs, with PAR2-mutant mice displaying significantly higher Arg-1 expression than their WT counterparts. These findings further implicate PAR2 in regulating fibrotic pathways, mainly through its influence on Arg-1 expression and the associated metabolic reprogramming that drives collagen synthesis.

In the current and prior studies, differences in the response to MWCNTs and HDM extract co-exposure are evident between PAR2-mutant versus complete PAR2 KO mice [6]. One possible explanation for the differences is the residual PAR2 activity in PAR2-mutant mice. Unlike complete knockout models where PAR2 signaling is entirely abrogated, partial deletion of PAR2 may allow for truncated or modified expression of PAR2, as shown via genotyping in Fig. 1. It has been well documented that modified GPCRs possess functionality in agonist binding, receptor activation, and interaction with cognate G proteins depending on the genetic alteration [29, 51, 52]. Considering PAR2 contains numerous activation residues, genetic modification of the receptor may change the affinity of a given ligand over another, resulting in biased or altered signaling [22, 28, 53]. Therefore, a mutated PAR2 receptor may continue to influence Arg-1 production through different signaling pathways compared to total PAR2 knockout models. However, there is currently no information on PAR2 protein in the PAR2-mutant mouse model, due in part to the lack of reliable PAR2 antibodies for Western blotting. On the other hand, Damiano and colleagues reported that the same PAR2-mutant mice used in our current study did not produce any detectable *Par2* mRNA in kidney or small intestine as determined by Northern blotting, which suggests that these mice would produce no PAR2 protein [31]. However, the possibility remains that the *Par2* cDNA used in the Northern blotting experiment in that paper did not recognize any putative mutated *Par2* mRNA. Therefore, the identity of *Par2* mRNA or PAR2 protein in the PAR2-mutant mice remains to be established if indeed they exist at all. Another potential explanation lies in genetic compensation mechanisms, in which the partial loss of function for a given receptor molecule triggers the upregulation of alternative genes or pathways that compensate for the deficiency [46, 54]. A similar scenario may exist, leading to Arg-1 upregulation in the PAR2-mutant mice, a response that does not occur in total PAR2 knockout models because those compensatory mechanisms are lost or not activated.

Our findings emphasize the complex role of PAR2 in allergic lung disease and fibrogenesis. While both PAR2-mutant and PAR2 KO models demonstrate the receptor's involvement in airway fibrosis, significant differences emerge in their regulation of key events, such as the regulation of Arg-1 production. Notably, the substantial upregulation of Arg-1 in PAR2-mutant mice, as opposed to its downregulation in complete PAR2 knockout models, suggests that residual PAR2 activity may influence alternative or compensatory signaling pathways. These results highlight that PAR2 genetic models share commonalities but also differ in the extent of receptor functionality and pathway engagement, leading to variations in disease outcomes. Interestingly, airway fibrosis was reduced despite elevated Arg-1 in PAR2-mutant mice, mirroring the effects seen in PAR2 KO mice in which Arg-1 is downregulated. This indicates that additional factors beyond Arg-1 contribute to fibrogenic outcomes. Understanding these differences is crucial for interpreting experimental data and the broader application of PAR2-targeted therapies for allergic lung disease and pulmonary fibrosis. Our research has the potential to impact the development of these therapies significantly. Future studies investigating the compensatory mechanisms in PAR2-mutant versus knockout models may shed light on the full spectrum of PAR2's role in lung pathology.

Conclusion

This study aimed to elucidate the role and functionality of PAR2 in the exacerbation of allergic lung disease and fibrogenesis following co-exposure to MWCNTs and HDM extract using a PAR2-mutant mouse model. Our investigation demonstrates that while partial gene deletion of PAR2 does not significantly mediate eosinophilic inflammation, it plays an important role in the development of airway fibrosis. Notably, we observed that both WT and PAR2-mutant displayed increased airway collagen following co-exposure to MWCNTs and HDM extract. However, PAR2-mutant mice showed significantly less airway collagen deposition and *Col1a1* mRNA, yet greater *Arg-1* mRNA and protein expression than WT mice. The reduced airway fibrosis in PAR2-mutant mice is similar to our previous observation of PAR2 KO mice with total gene deletion [6]. However, increased Arg-1 protein in PAR2-mutant mice in the present study contrasts with our previous work with PAR2 KO mice, which displayed reduced Arg-1 expression after co-exposure to MWCNTs and HDM extract [6]. In summary, our study using PAR2-mutant mice provides further evidence for PAR2 as a mediator of airway fibrogenesis during allergic lung disease, yet the differential expression of Arg-1 in PAR2-mutant versus PAR2 KO mice highlights potentially important differences in a key metabolic enzyme involved in fibrogenesis.

Abbreviations

PAR2	Protease-activated receptor-2
MWCNT	Multi-walled carbon nanotubes
HDM	House dust mite
LPS	Lipopolysaccharide
BALF	Bronchoalveolar lavage fluid
LDH	Lactate dehydrogenase
ENM	Engineered nanomaterial
CXCL1	C-X-C motif chemokine ligand 1
CCL11	C–C motif chemokine ligand 11 (eotaxin)
ARG-1	Arginase-1
OPA	Oropharyngeal aspiration

STAT-6 Signal transducer and activator of transcription 6
TLR4 Toll-like receptor 4

Supplementary Information

The online version contains supplementary material available at https://doi.org/10.1186/s12931-025-03168-y.

Supplementary Material 1.

Supplementary Material 2.

Author contributions

LJT, SA, and JCB designed the experiments and participated in data interpretation. LJT, RDB, SA, and JCB performed the experiments and performed the data analysis. LJT and JCB wrote the manuscript. All other coauthors edited the manuscript.

Funding

This work was funded by National Institute of Environmental Health Sciences (NIEHS) grant R01ES032443 and NIEHS grant P30ES025128. LJT and RDB were partially supported by NIEHS Training Grant T32ES007046.

Availability of data and materials

No datasets were generated or analysed during the current study.

Declarations

Ethics approval and consent to participate

The animal study was approved by the North Carolina State University Animal Care and Use Committee (NCSU IACUC protocol #19-681).

Consent for publication

Not applicable.

Competing interests

The authors declare no competing interests.

Author details

[1]Toxicology Program, Department of Biological Sciences, North Carolina State University, Raleigh, NC, USA. [2]UNC Blood Research Center, Department of Pathology and Laboratory Medicine, School of Medicine, University of North Carolina at Chapel Hill, Chapel Hill, NC, USA.

Received: 22 November 2024 Accepted: 24 February 2025
Published online: 08 March 2025

References

1. Hartert TV, Peebles RS Jr. Epidemiology of asthma: the year in review. Curr Opin Pulm Med. 2000;6(1):4–9.
2. Xepapadaki P, Bachert C, Finotto S, Jartti T, Konstantinou GN, Kiefer A, Kowalski M, Lewandowska-Polak A, Lukkarinen H, Roumpedaki E, Sobanska A. Contribution of repeated infections in asthma persistence from preschool to school age: design and characteristics of the PreDicta cohort. Pediatr Allergy Immunol. 2018;29(4):383–93.
3. Earl CS, An SQ, Ryan RP. The changing face of asthma and its relation with microbes. Trends Microbiol. 2015;23(7):408–18.
4. Youssouf H, Liousse C, Roblou L, Assamoi EM, Salonen RO, Maesano C, Banerjee S, Annesi-Maesano I. Non-accidental health impacts of wildfire smoke. Int J Environ Res Public Health. 2014;11(11):11772–804.
5. Liu X, Lessner L, Carpenter DO. Association between residential proximity to fuel-fired power plants and hospitalization rate for respiratory diseases. Environ Health Perspect. 2012;120(6):807–10.
6. Lee HY, You DJ, Taylor-Just A, Tisch LJ, Bartone RD, Atkins HM, Ralph LM, Antoniak S, Bonner JC. Role of the protease-activated receptor-2 (PAR2) in the exacerbation of house dust mite-induced murine allergic lung disease by multi-walled carbon nanotubes. Part Fibre Toxicol. 2023;20(1):32.
7. Duke KS, Bonner JC. Mechanisms of carbon nanotube-induced pulmonary fibrosis: a physicochemical characteristic perspective. Wiley Interdiscip Rev Nanomed Nanobiotechnol. 2018;10(3): e1498.
8. Cha C, Shin SR, Annabi N, Dokmeci MR, Khademhosseini A. Carbon-based nanomaterials: multifunctional materials for biomedical engineering. ACS Nano. 2013;7(4):2891–7.
9. Ryman-Rasmussen JP, Cesta MF, Brody AR, Shipley-Phillips JK, Everitt JI, Tewksbury EW, Moss OR, Wong BA, Dodd DE, Andersen ME, Bonner JC. Inhaled carbon nanotubes reach the subpleural tissue in mice. Nat Nanotechnol. 2009;4(11):747–51.
10. Bonner JC. Nanoparticles as a potential cause of pleural and interstitial lung disease. Proc Am Thorac Soc. 2010;7(2):138–41.
11. Mitchell LA, Lauer FT, Burchiel SW, McDonald JD. Mechanisms for how inhaled multiwalled carbon nanotubes suppress systemic immune function in mice. Nat Nanotechnol. 2009;4(7):451–6.
12. Ihrie MD, Taylor-Just AJ, Walker NJ, Stout MD, Gupta A, Richey JS, Hayden BK, Baker GL, Sparrow BR, Duke KS, Bonner JC. Inhalation exposure to multi-walled carbon nanotubes alters the pulmonary allergic response of mice to house dust mite allergen. Inhalation Toxicol. 2019;31(5):192–202.
13. Shipkowski KA, Taylor AJ, Thompson EA, Glista-Baker EE, Sayers BC, Messenger ZJ, Bauer RN, Jaspers I, Bonner JC. An allergic lung microenvironment suppresses carbon nanotube-induced inflammasome activation via STAT6-dependent inhibition of caspase-1. PLoS ONE. 2015;10(6): e0128888.
14. Bartone RD, Tisch LJ, Dominguez J, Payne CK, Bonner JC. House dust mite proteins adsorb on multiwalled carbon nanotubes forming an allergen corona that intensifies allergic lung disease in mice. ACS Nano. 2024;18(38):26215–32.
15. Janeway CA Jr, Medzhitov R. Innate immune recognition. Annu Rev Immunol. 2002;20(1):197–216.
16. Cocks TM, Moffatt JD. Protease-activated receptor-2 (PAR2) in the airways. Pulm Pharmacol Ther. 2001;14(3):183–91.
17. Chakraborty K, Bhattacharyya A. Role of proteases in inflammatory lung diseases. Proteases Health Dis. 2013;7:361–85.
18. Rallabhandi P, Nhu QM, Toshchakov VY, Piao W, Medvedev AE, Hollenberg MD, Fasano A, Vogel SN. Analysis of proteinase-activated receptor 2 and TLR4 signal transduction: a novel paradigm for receptor cooperativity. J Biol Chem. 2008;283(36):24314–25.
19. Sun G, Stacey MA, Schmidt M, Mori L, Mattoli S. Interaction of mite allergens Der p3 and Der p9 with protease-activated receptor-2 expressed by lung epithelial cells. J Immunol. 2001;167(2):1014–21.
20. Asokananthan N, Graham PT, Stewart DJ, Bakker AJ, Eidne KA, Thompson PJ, Stewart GA. House dust mite allergens induce proinflammatory cytokines from respiratory epithelial cells: the cysteine protease allergen, Der p 1, activates protease-activated receptor (PAR)-2 and inactivates PAR-1. J Immunol. 2002;169(8):4572–8.
21. Schmidlin F, Amadesi S, Dabbagh K, Lewis DE, Knott P, Bunnett NW, Gater PR, Geppetti P, Bertrand C, Stevens ME. Protease-activated receptor 2 mediates eosinophil infiltration and hyperreactivity in allergic inflammation of the airway. J Immunol. 2002;169(9):5315–21.
22. Heuberger DM, Schuepbach RA. Protease-activated receptors (PARs): mechanisms of action and potential therapeutic modulators in PAR-driven inflammatory diseases. Thromb J. 2019;17(1):4.
23. Rayees S, Rochford I, Joshi JC, Joshi B, Banerjee S, Mehta D. Macrophage TLR4 and PAR2 signaling: role in regulating vascular inflammatory injury and repair. Front Immunol. 2020;11:2091.
24. Vliagoftis H, Asaduzzaman M, Davidson C. Functional inhibition of PAR2 prevents inflammation and tissue remodelling in a long-Term model of cockroach-mediated allergic airway inflammation. J Allergy Clin Immunol. 2015;135(2):AB62.
25. Su X, Matthay MA. Role of protease activated receptor 2 in experimental acute lung injury and lung fibrosis. Anat Rec Adv Integr Anat Evol Biol. 2009;292(4):580–6.
26. Lindner JR, Kahn ML, Coughlin SR, Sambrano GR, Schauble E, Bernstein D, Foy D, Hafezi-Moghadam A, Ley K. Delayed onset of inflammation in protease-activated receptor-2-deficient mice. J Immunol. 2000;165(11):6504–10.

27. Lin KW, Park J, Crews AL, Li Y, Adler KB. Protease-activated receptor-2 (PAR-2) is a weak enhancer of mucin secretion by human bronchial epithelial cells in vitro. Int J Biochem Cell Biol. 2008;40(6–7):1379–88.
28. Kennedy AJ, Ballante F, Johansson JR, Milligan G, Sundström L, Nordqvist A, Carlsson J. Structural characterization of agonist binding to protease-activated receptor 2 through mutagenesis and computational modeling. ACS Pharmacol Transl Sci. 2018;1(2):119–33.
29. Schöneberg T, Liebscher I. Mutations in G protein–coupled receptors: mechanisms, pathophysiology and potential therapeutic approaches. Pharmacol Rev. 2021;73(1):89–119.
30. Taylor-Just AJ, Ihrie MD, Duke KS, Lee HY, You DJ, Hussain S, Kodali VK, Ziemann C, Creutzenberg O, Vulpoi A, Turcu F. The pulmonary toxicity of carboxylated or aminated multi-walled carbon nanotubes in mice is determined by the prior purification method. Part Fibre Toxicol. 2020;17:1–8.
31. Damiano BP, Cheung WM, Santulli RJ, Fung-Leung WP, Ngo K, Richard DY, Darrow AL, Derian CK, de Garavilla L, Andrade-Gordon P. Cardiovascular responses mediated by protease-activated receptor-2 (PAR-2) and thrombin receptor (PAR-1) are distinguished in mice deficient in PAR-2 or PAR-1. J Pharmacol Exp Ther. 1999;288(2):671–8.
32. Gunther RC, Bharathi V, Miles SD, Tumey LR, Schmedes CM, Tatsumi K, Bridges MD, Martinez D, Montgomery SA, Beck MA, Camerer E, Mackman N, Antoniak S. Myeloid protease-activated receptor-2 contributes to influenza A virus pathology in mice. Front Immunol. 2021;12: 791017.
33. Antoniak S, Rojas M, Spring D, Bullard TA, Verrier ED, Blaxall BC, Mackman N, Pawlinski R. Protease-activated receptor 2 deficiency reduces cardiac ischemia/reperfusion injury. Arterioscler Thromb Vasc Biol. 2010;30:2136–42.
34. Chung H, Ramachandran R, Hollenberg MD, Muruve DA. Proteinase-activated receptor-2 transactivation of epidermal growth factor and transforming growth factor-β receptor signaling pathways contributes to renal fibrosis. J Biol Chem. 2013;288(52):37319–31.
35. Sayers BC, Taylor AJ, Glista-Baker EE, Shipley-Phillips JK, Dackor RT, Edin ML, Lih FB, Tomer KB, Zeldin DC, Langenbach R, Bonner JC. Role of cyclooxygenase-2 in exacerbation of allergen-induced airway remodeling by multiwalled carbon nanotubes. Am J Respir Cell Mol Biol. 2013;49(4):525–35.
36. Ihrie MD, Duke KS, Shipkowski KA, You DJ, Lee HY, Taylor-Just AJ, Bonner JC. STAT6-dependent exacerbation of house dust mite-induced allergic airway disease in mice by multi-walled carbon nanotubes. NanoImpact. 2021;22: 100309.
37. Reader JR, Tepper JS, Schelegle ES, Aldrich MC, Putney LF, Pfeiffer JW, Hyde DM. Pathogenesis of mucous cell metaplasia in a murine asthma model. Am J Pathol. 2003;162(6):2069–78.
38. Wilson JW, Bamford TL. Assessing the evidence for remodelling of the airway in asthma. Pulm Pharmacol Ther. 2001;14(3):229–47.
39. Alberts B, Johnson A, Lewis J, Raff M, Roberts K, Walter P. The airways and the gut. In: Molecular biology of the cell. 4th ed. Garland Science; 2002.
40. Chi L, Li Y, Stehno-Bittel L, Gao J, Morrison DC, Stechschulte DJ, Dileepan KN. Interleukin-6 production by endothelial cells via stimulation of protease-activated receptors is amplified by endotoxin and tumor necrosis factor-α. J Interferon Cytokine Res. 2001;21(4):231–40.
41. Nhu QM, Shirey KA, Pennini ME, Stiltz J, Vogel SN. Proteinase-activated receptor 2 activation promotes an anti-inflammatory and alternatively activated phenotype in LPS-stimulated murine macrophages. Innate Immun. 2012;18(2):193–203.
42. Liang HP, Kerschen EJ, Hernandez I, Basu S, Zogg M, Botros F, Jia S, Hessner MJ, Griffin JH, Ruf W, Weiler H. EPCR-dependent PAR2 activation by the blood coagulation initiation complex regulates LPS-triggered interferon responses in mice. Blood J Am Soc Hematol. 2015;125(18):2845–54.
43. Zhuo X, Wu Y, Fu X, Liang X, Xiang Y, Li J, Mao C, Jiang Y. The Yin-Yang roles of protease-activated receptors in inflammatory signalling and diseases. FEBS J. 2022;289(14):4000–20.
44. Bhatia M, Zemans RL, Jeyaseelan S. Role of chemokines in the pathogenesis of acute lung injury. Am J Respir Cell Mol Biol. 2012;46(5):566–72.
45. Nagarkar DR, Wang Q, Shim J, Zhao Y, Tsai WC, Lukacs NW, Sajjan U, Hershenson MB. CXCR2 is required for neutrophilic airway inflammation and hyperresponsiveness in a mouse model of human rhinovirus infection. J Immunol. 2009;183(10):6698–707.
46. Wang Y, Zhao J, Zhang H, Wang CY. Arginine is a key player in fibroblasts during the course of IPF development. Mol Ther. 2021;29(4):1361–3.
47. Krane SM. The importance of proline residues in the structure, stability and susceptibility to proteolytic degradation of collagens. Amino Acids. 2008;35(4):703–10.
48. Roque W, Romero F. Cellular metabolomics of pulmonary fibrosis, from amino acids to lipids. Am J Physiol Cell Physiol. 2021;320(5):C689–95.
49. Zhang L, Qu S, Wang L, Wang C, Yu Q, Zhang Z, Diao Y, Zhang B, Li Y, Shi Y, Wang P. Tianlongkechuanling inhibits pulmonary fibrosis through down-regulation of arginase-ornithine pathway. Front Pharmacol. 2021;12: 661129.
50. Kitowska K, Zakrzewicz D, Königshoff M, Chrobak I, Grimminger F, Seeger W, Bulau P, Eickelberg O. Functional role and species-specific contribution of arginases in pulmonary fibrosis. Am J Physiol Lung Cell Mol Physiol. 2008;294(1):L34-45.
51. Ulloa-Aguirre A, Zariñán T, Dias JA, Conn PM. Mutations in G protein-coupled receptors that impact receptor trafficking and reproductive function. Mol Cell Endocrinol. 2014;382(1):411–23.
52. Lee-Rivera I, López E, López-Colomé AM. Diversification of PAR signaling through receptor crosstalk. Cell Mol Biol Lett. 2022;27(1):77.
53. Maryanoff BE, Santulli RJ, McComsey DF, Hoekstra WJ, Hoey K, Smith CE, Addo M, Darrow AL, Andrade-Gordon P. Protease-activated receptor-2 (PAR-2): structure-function study of receptor activation by diverse peptides related to tethered-ligand epitopes. Arch Biochem Biophys. 2001;386(2):195–204.
54. El-Brolosy MA, Stainier DY. Genetic compensation: a phenomenon in search of mechanisms. PLoS Genet. 2017;13(7): e1006780.

Publisher's Note